PROCEEDINGS OF SPIE

SPIEDigitalLibrary.org/conference-proceedings-of-spie

Background studies for ATHENA: status of the activities at IAAT

E. Perinati, S. Diebold, A. Guzman, A. Santangelo, C. Tenzer

E. Perinati, S. Diebold, A. Guzman, A. Santangelo, C. Tenzer, "Background studies for ATHENA: status of the activities at IAAT," Proc. SPIE 9905, Space Telescopes and Instrumentation 2016: Ultraviolet to Gamma Ray, 990565 (18 July 2016); doi: 10.1117/12.2231599

SPIE.

Event: SPIE Astronomical Telescopes + Instrumentation, 2016, Edinburgh, United Kingdom

Downloaded From: https://www.spiedigitallibrary.org/conference-proceedings-of-spie on 2/28/2019 Terms of Use: https://www.spiedigitallibrary.org/terms-of-use

Background studies for ATHENA: status of the activities at IAAT

E. Perinati*, S. Diebold, A. Guzman, A. Santangelo and C. Tenzer
IAAT-Institute für Astronomie und Astrophysik, Universität Tübingen, Germany

ABSTRACT

We present an update on the status of the activities at IAAT for the assessment of the background and optimization of the camera design in the context of ATHENA/WFI.

1. INTRODUCTION

The Wide Field Imager (WFI) [1] is one of the two focal plane instruments proposed for the ESA's Advanced Telescope for High ENergy Astrophysics (ATHENA) [2]. It is a Si-based detector developed at MPE, structured in two parts (Fig. 1): a large chip with 40'x 40' FOV mounted in the focus of the telescope, divided into four quadrants 512x512 pixel each; and a smaller fast chip 64x64 pixel mounted defocused by 35 mm, for the observation of bright sources. Each pixel is a DEPFET, i.e. an active sensor consisting of a low capacitance p-channel MOSFET implanted on a high resistivity sideward depleted n-type Si substrate, allowing for in-situ amplification of the charge generated by the absorption of X-rays, which results in fast low noise readout without charge transfer. The WFI will provide sensitive wide field imaging in the range 0.1-15 keV, with moderate spectral resolution (<150 eV @6 keV), high time resolution (~8 μsec window mode, ~1.3 msec full frame) and high count-rate capacity (~1 Crab), complementing the exquisite spectral capabilities of the X-ray Integral Field Unit (XIFU) [3]. In this paper we report on the background studies in progress at IAAT, one of the institutes collaborating with MPE in the effort of predicting by simulations the various components of the instrumental background and optimizing the camera design to improve the sensitivity of the detector as well as the strategies for the monitoring and the rejection of the background in-flight.

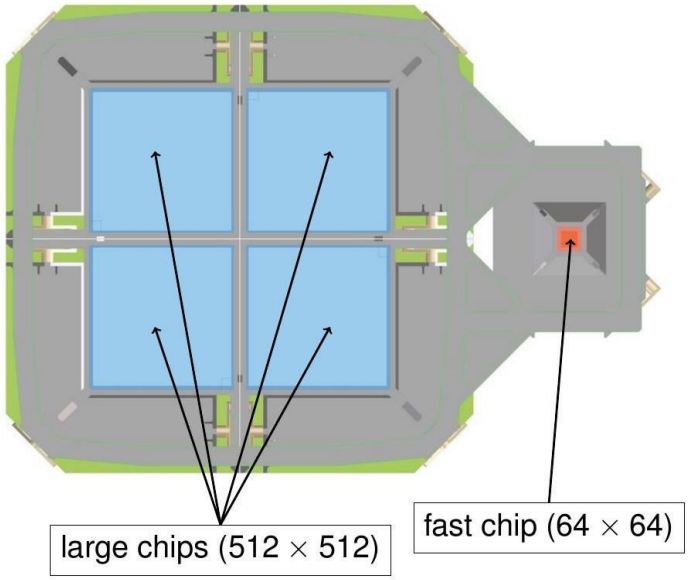

Figure 1. The proposed ATHENA/WFI instrument features a large detector divided into four quadrants (512x512 pixel each) mounted in the focus of the telescope and a smaller (64x64 pixel) fast detector defocused by 35 mm. (credit:MPE)

*emanuele.perinati@uni-tuebingen.de; tel. +49-7071-29-73457

Space Telescopes and Instrumentation 2016: Ultraviolet to Gamma Ray, edited by
Jan-Willem A. den Herder, Tadayuki Takahashi, Marshall Bautz, Proc. of SPIE Vol. 9905, 990565
© 2016 SPIE · CCC code: 0277-786X/16/$18 · doi: 10.1117/12.2231599

Downloaded From: https://www.spiedigitallibrary.org/conference-proceedings-of-spie on 2/28/2019
Terms of Use: https://www.spiedigitallibrary.org/terms-of-use

2. PARTICLE BACKGROUND

The level of instrumental background limits the sensitivity achievable by the WFI, and it is one of the aspects driving the design of the camera. At lower energies (<2 keV) the background is expected dominated by the diffused cosmic X-rays focused by the telescope. At higher energies the dominant contribution is expected from the interaction of environmental charged particles, mainly high energy protons. A count-rate of $5 \cdot 10^{-3}$ cts/cm^2/sec/keV has been assumed as a requirement for both the WFI and the XIFU, a value quite similar to the close-pos continuum measured by the pnCCD aboard XMM-Netwon, orbiting in an environment where the galactic fluxes of charged particles are expected not too different from those at L2. Considering the larger effective area of ATHENA compared to XMM, an XMM-like particle background would still guarantee a significant improvement in sensitivity. As the requirement is an upper limit, a count-rate below that value would be a goal and efforts are made to optimize the configuration and the rejection algorithms, in order to minimize the expected rate of false counts generated by environmental radiation.

The residual background will be mostly due to secondary particles originating from structural components at the focal plane, as false counts produced by the direct interaction of primary protons with the detector can be rejected with very high efficiency (>99.5%). This is because the WFI depleted volume is relatively thick (450 μm) and in most cases impinging protons will travel in it paths longer than 40 μm, therefore even the minimum ionizing ones, that in Si have an average energy loss of ~0.4 keV/μm (Fig. 2), will be depositing an amount of energy >15 keV. Protons impinging at angles small enough may be able to deposit <15 keV in pixels belonging to the very peripheral part of the detector, where the profile of the point spread function gets flattened, so that these events actually are not an issue.

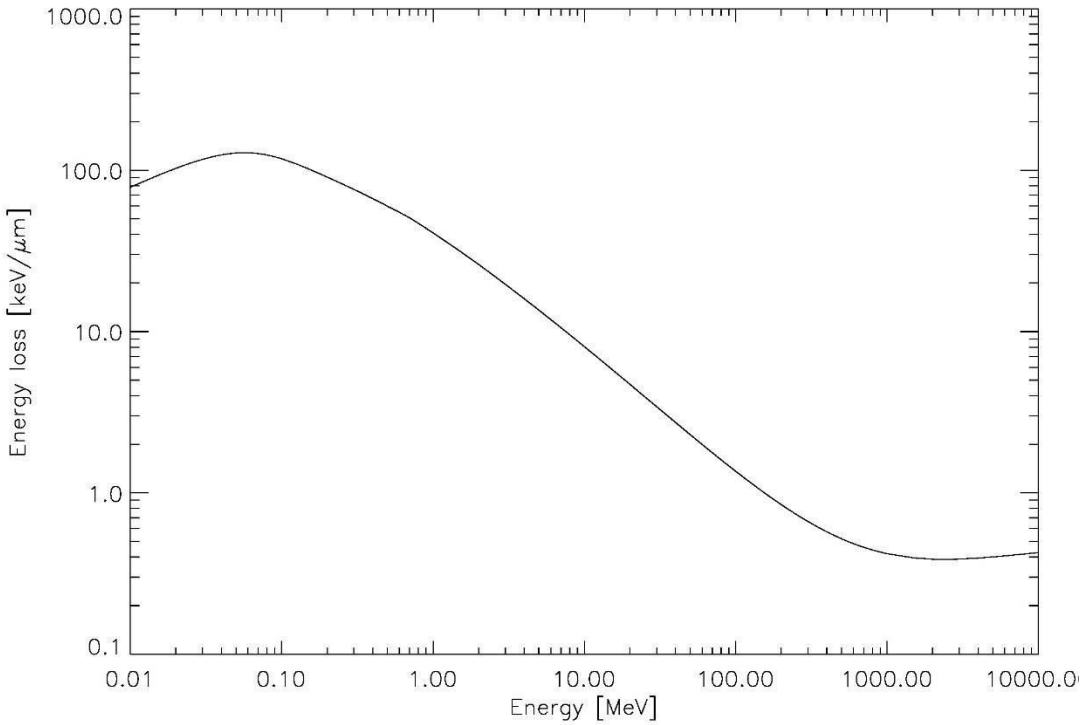

Figure 2. Average energy loss of protons in Si

The WFI configuration envisages a 4 cm thick Al shield around the detector to cut environmental protons up to ~110 MeV. Although these protons are only a small fraction of the overall environmental flux, they are the most harmful having a higher non-ionizing energy loss (NIEL) in Si (Fig. 3), that can lead to the generation of defects in the crystal by atomic displacement. On the other hand, the shield acts as a source of background, generating secondary particles, to a larger extent electrons and X-rays, when energetic protons strike it. Softer electrons ejected from the surface of the shield with

Downloaded From: https://www.spiedigitallibrary.org/conference-proceedings-of-spie on 2/28/2019
Terms of Use: https://www.spiedigitallibrary.org/terms-of-use

an energy in the band give valid absorption patterns that cannot be discriminated by those of signal X-rays. Higher energy electrons can also contribute to the background if they undergo backscattering at the surface, penetrating into the sensitive volume only over a small distance before being reflected, then depositing just a small fraction of their energy. Soft X-rays can be generated inside the shield by Bremsstrahlung, clearly they also give absorption patterns that cannot be distinguished from those of signal X-rays. X-rays with energy >15 keV can generate false counts by Compton scattering in the Si crystal. Energetic protons can excite fluorescence as well, resulting in the emission of X-rays at characteristic energies producing spectral features in the detected background spectrum. In the case of an Al shield a line at ~1.6 keV is expected.

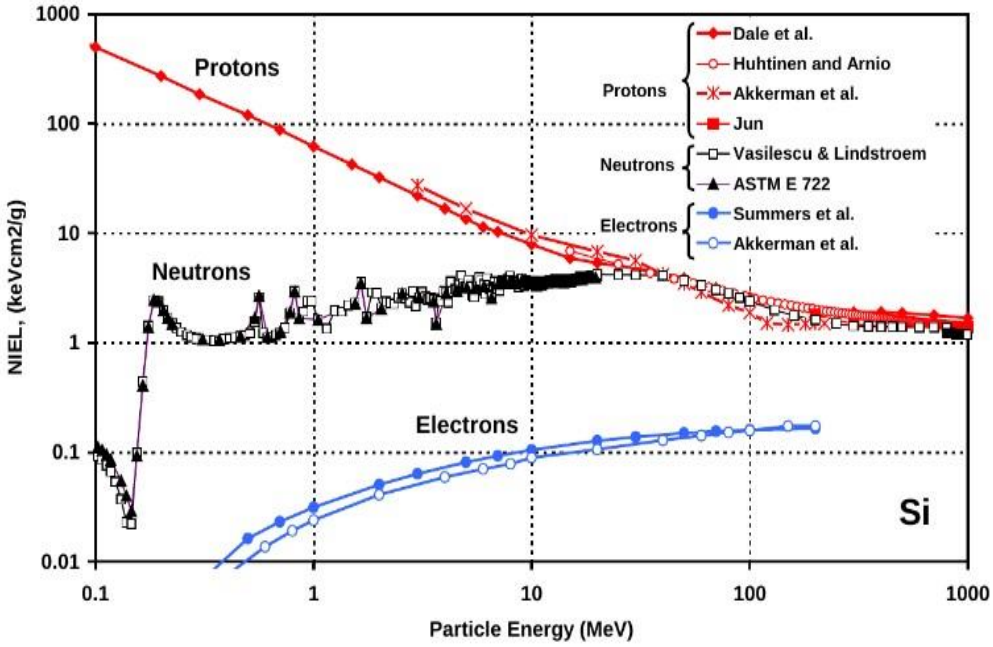

Figure 3. NIEL of protons,electrons and neutrons in Si as a function of energy (credit:ESA)

2.1 Geant4 simulation: basic camera head

In this section we report results of simulations done in Geant4 10.01.p02 using the basic camera head configuration, i.e. the shield with the detector floating inside (sub-structures, e.g. baffle, filter-wheel, etc., are not included at this stage), as shown in Fig 4. The shield is a 4 cm thick Al box, the detector is a Si slab 15x15 cm with 90 nm Al plating on top. Although it is a simplified description, it is sufficient for a first order estimate of the level of background to be expected on the detector, as sub-structures would contribute only to a lesser extent.

Downloaded From: https://www.spiedigitallibrary.org/conference-proceedings-of-spie on 2/28/2019
Terms of Use: https://www.spiedigitallibrary.org/terms-of-use

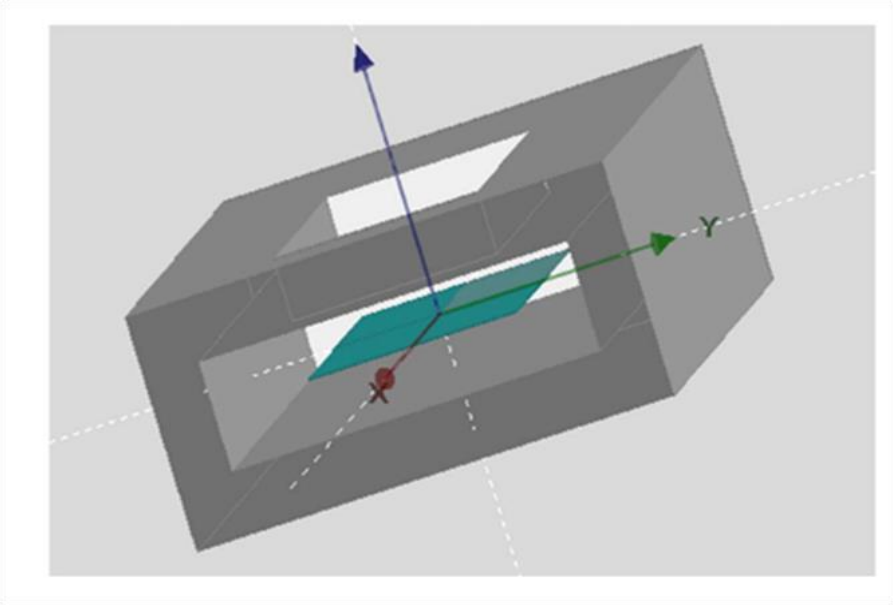

Figure 4. The basic geometry used in these simulations: a 4 cm thick Al box with a Si slab inside (credit:MPE)

We simulated the residual background originating from the expected average flux of galactic protons at L2 [4]. It consists mostly of secondary electrons (~54%) and X-rays (~40%), with a minor contribution (~4%) from elastic scattering in the Si lattice by spallation neutrons. There is ~2% of events produced by the direct interaction of protons with the detector, these events affect only pixels at the edges of the detector, as previously explained. Due to the FOV aperture, the lower part of the shield contributes more background (~60%) than the upper part (~40%). The background level decreases with energy (Fig. 4) and at energies >7 keV it is about within the required value. To reduce the level at energies <7 keV we investigated the application of a passivation layer on the non-illuminated side of the detector. The layer works primarily by cutting the softer electrons emitted from the lower part of the shield, which can be fully absorbed. To prevent electrons up to 15 keV from reaching the sensitive volume a few micron thick layer should be used, the actual thickness depends on the material. A technically feasible passivation may consist of 3 □m benzocyclobutene (BCB) coating. The red line in Fig. 4 shows the effect on the background. The layer does not add background as no gap is left in between, so that all secondaries generated in it can be rejected with the same efficiency as the primary protons that excite them. Unavoidably, the layer introduces a shift in energy of the incoming electron flux, so that on one hand incoming electrons up to 15 keV get stopped, on the other hand incoming electrons >15 keV may undergo enough energy degradation traversing the layer to emerge with an energy in the band. However, as the flux of secondary electrons ejected from the shield decreases with energy, as shown in Fig.5, the resulting balance is positive, i.e. the continuum effectively reduces by ~20% on average over the entire band, and by more than 30% at energies <7 keV, where the percentage of electrons in the background is higher. As a result, a nearly flat level ~$5 \cdot 10^{-3}$ cts/cm^2/sec/keV is achieved over the entire band. Notice that 90 nm Al and 3 μm BCB have both a transmissivity ~90% at 1.6 keV, hence the background spectrum still contains a prominent spectral feature induced by the characteristic fluorescence emission from the Al shield. To get rid of this disturbing feature, an internal layer mounted in front of the shield will be used. The game is to select properly material and thickness to achieve a transmissivity less than 1% at 1.6 keV without introducing any significant additional contribution to the background. Therefore, a low-Z material should be preferred, e.g. 1 mm thickness of Be, B or C could do the job. However, the absorbing layer may be structured in a more elaborated way, as a combination of high-Z and low-Z materials, to possibly decrease further the continuum level as well. We remark that, including sub-structures in the camera configuration and adding galactic α-particles end electrons in input to the simulations, an increase by ~20% of the background may be expected. The non-X-ray-background induced from the cosmic X-ray background is under investigation and not included in the study presented here.

Downloaded From: https://www.spiedigitallibrary.org/conference-proceedings-of-spie on 2/28/2019
Terms of Use: https://www.spiedigitallibrary.org/terms-of-use

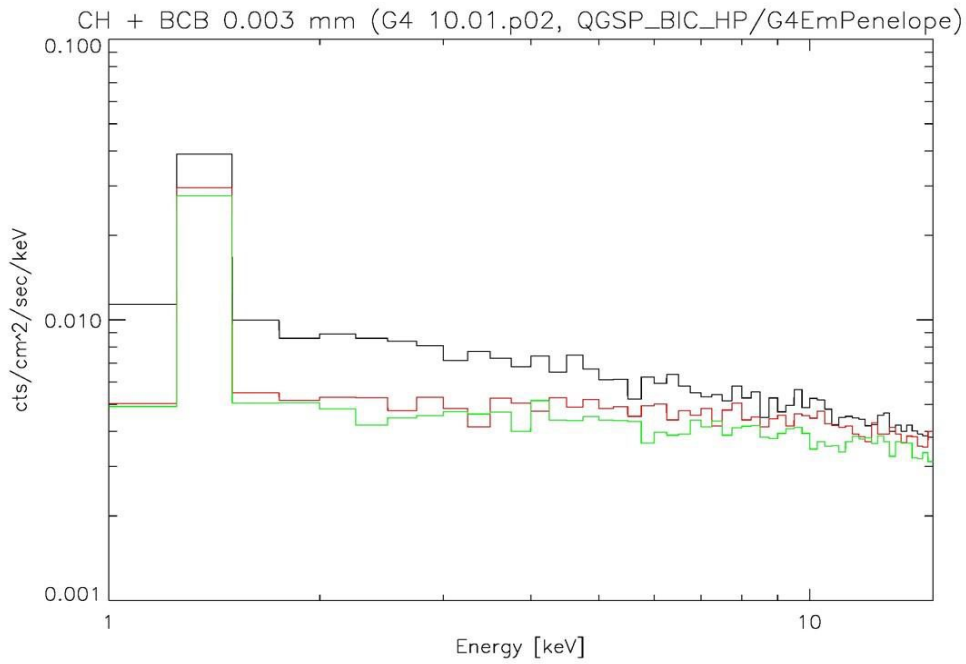

Figure 4. Simulated WFI background induced by galactic protons in the basic camera head configuration:the black line is the level corresponding to a detector without passivation floating inside the Al box. The red line is the level corresponding to a detector with 3 μm BCB passivation on the non-illuminated side. The green line is the level corresponding to a detector with passivation, positioned 1 cm closer to the opening.

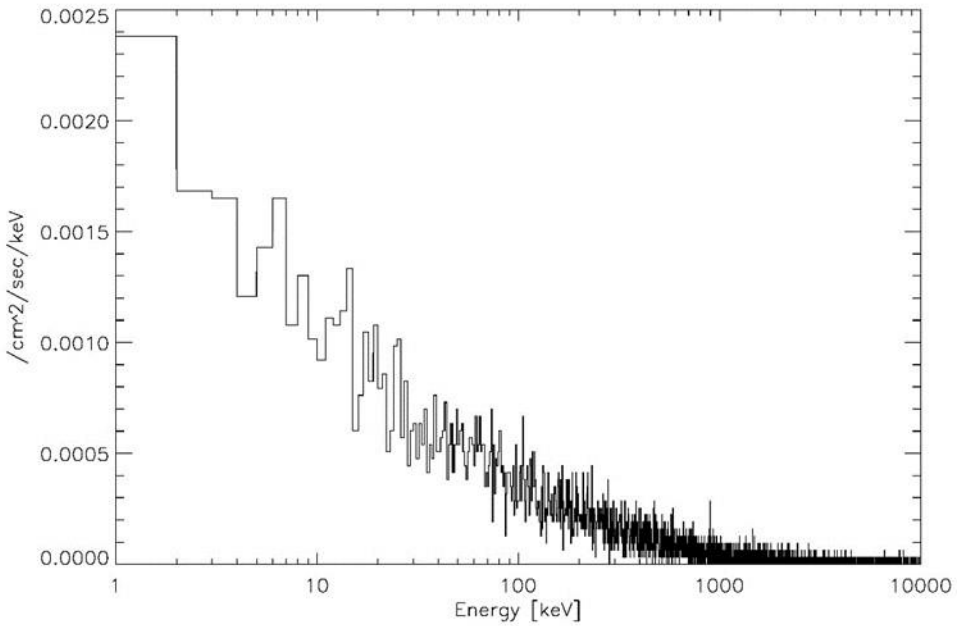

Figure 5. Simulated flux of secondary electrons onto the non-illuminated side of the detector

Downloaded From: https://www.spiedigitallibrary.org/conference-proceedings-of-spie on 2/28/2019
Terms of Use: https://www.spiedigitallibrary.org/terms-of-use

2.2 Geant4 simulation: optical blocking filter

One of the sub-structures present in the design of the WFI camera is the optical blocking filter (OBF) needed to reduce the load of visible/UV light to the detector. The current OBF baseline prefigures an external filter 30 nm Al+150 nm Polymide [4] coupled to a filter (90 nm Al) deposited on-chip. The external filter will be positioned above WFI at a distance of a few cm from the detector plane. Although the contribution to the background from the filter alone is likely negligible, it is worth considering the overall effect of the filter and the mesh that is being investigated as a solution to mechanically sustain the filter. We studied the case of a squared mesh (Fig. 6) with the following specifications (provided by M. Barbera):

-size = 160x160 mm

-thickness = 250 μm

-width (i.e. spacing between celles) = 70 μm

-pitch (i.e. center-to-center distance between celles) = 3 mm

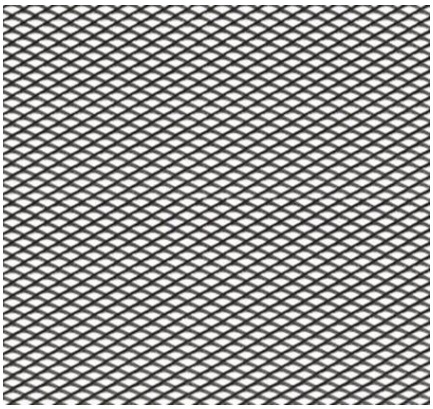

Figure 6. The simulated mesh

Three candidate materials have been initially considered: Al, Ti and stainless steel #316 (Fe 64%, Cr 18%, Ni 14%, Mo 2%, Mn 2%) . We simulated the excess background that a mesh positioned above the WFI at 12 cm distance would generate on the detector. Fig. 7 shows the resulting spectra. In all three cases, the excess continuum introduced by the mesh is negligible (<2% if referred to a flat level of $5 \cdot 10^{-3}$ cts/cm^2/sec/keV), however characteristic fluorescence lines are relatively pronounced and it might be desirable to avoid them.

Coating the mesh with 5 μm Au produces complete suppression of the fluorescence lines from the bulk material, although two small Au L-fluorescence features appear at ~9.7 keV and ~11.4 keV (Fig. 7). Coating the mesh with 7 μm Ag produces as well complete suppression of the fluorescence lines from the bulk material, and no fluorescence features from the coating are present in the spectrum (Fig. 7), being the Ag L-yield much smaller than that of Au. For a mesh in Ti 4 μm Ag is enough, for a mesh in Al 1 μm Ag is enough. As an alternative that could be worth some investigation, C-fibre is a lightweight, hard and very resistant material with a fluorescence yield much smaller than a metal, therefore no fluorescence features are present in the spectrum generated by a mesh in C-fibre (Fig. 7). Moreover, C-fibre has got also an X-ray transmissivity significantly higher than a metal, that it looks like as a better candidate material to fulfill the requirement on the throughput at 6-7 keV. Since it seems unlikely to find on the market C-fibre wire/rods with the requested specifications to build a crisscross mesh, an alternative way would be drilling a thin C-fibre sheet to open on it an array of celles. However, using conventional drilling techniques a wall of material as thin as ~100 μm between celles would most likely fail during the cutting loads, therefore we are currently exploring drilling by a laser beam and some tests will be performed soon.

Downloaded From: https://www.spiedigitallibrary.org/conference-proceedings-of-spie on 2/28/2019
Terms of Use: https://www.spiedigitallibrary.org/terms-of-use

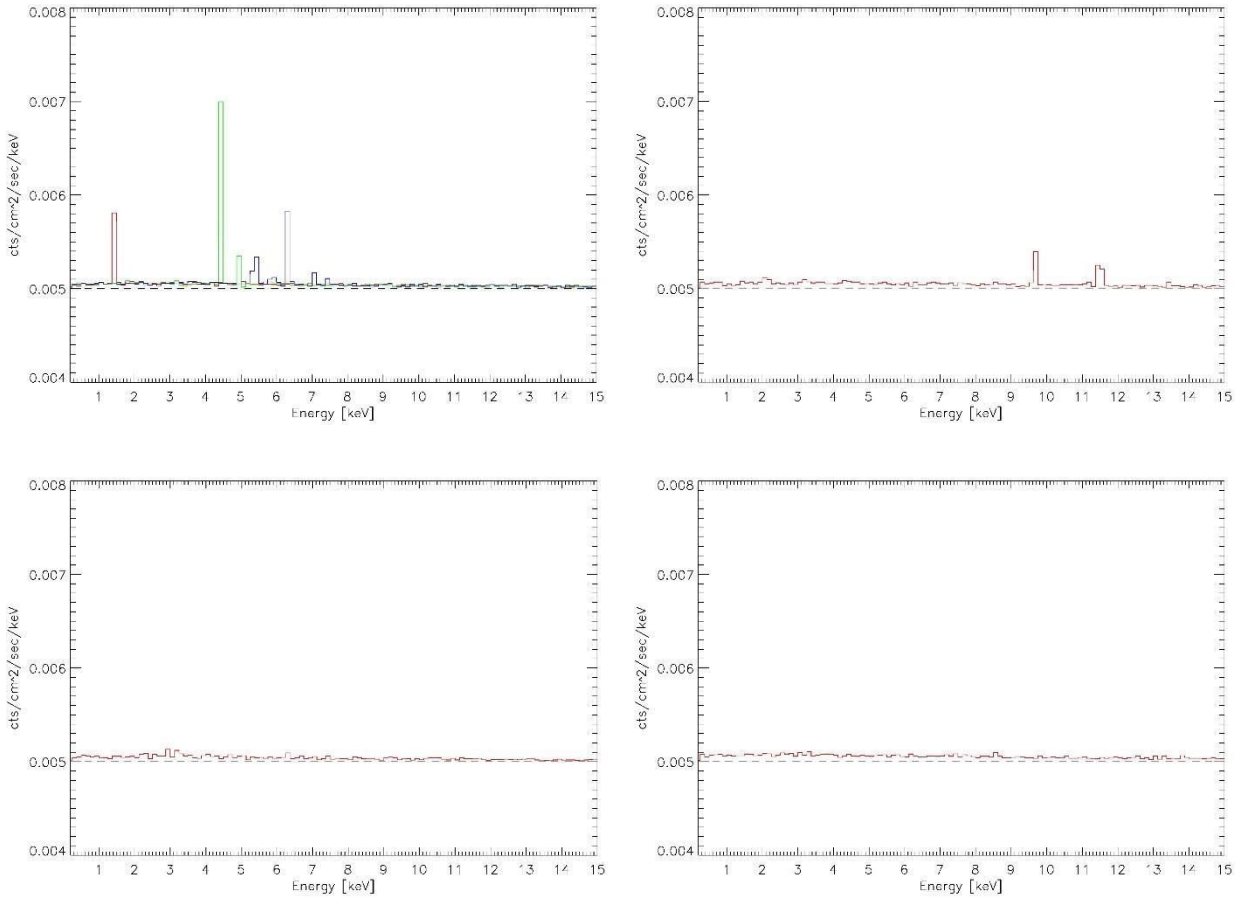

Figure 7. *Top left*: overall background expected mounting a mesh in Al (red line), Ti (green line) and stainless steel (blue line) above the WFI, assuming a flat baseline level of $5 \cdot 10^{-3}$ cts/cm^2/sec/keV withouth mesh The excess continuum introduced by the mesh is $<10^{-4}$ cts/cm^2/sec/keV, however characteristic K_α lines are relatively pronounced. *Top right*: bulk fluorescences can be completely absorbed by coating the mesh with 5 μm Au, although two small L-fluorescence features appear in the spectrum. *Bottom left*: coating with 7 μm Ag also produces complete suppression of the bulk fluorescences withouth introducing other features. *Bottom right*: no spectral features are present in the background of a mesh in C-fibre.

2.3 Soft protons

A 4 cm thickness of Al is able to stop on average protons up to 110 MeV. Therefore, environmental softer (< 10 MeV) protons with solar origin in principle would not be an issue, however they may be funneled to the focal plane through the telescope. This effect has been experienced by both Chandra [5] and XMM-Netwon [6]. Although the DEPFET detector developed for ATHENA is likely less susceptible to radiation damage than a CCD, as no charge transfer is applied, soft protons reaching the focal plane may contribute to increase the background level. As a matter of fact, quite a lot of XMM observations were strongly affected by soft protons. For this reason, a proton diverter is being investigated to reduce the possible flux of soft protons at the ATHENA focal plane well below the threshold of $5 \cdot 10^{-3}$ cts/cm^2/sec/keV. Two inputs would be helpful in this analysis: the expected flux of soft protons that will be entering the telescope from the environment and the properties of proton transmissivity of the telescope. While the first is largely uncertain due to the lack of radiation monitors at L2 in the softer energy range, there are theoretical models that describe the physics underlying the reflection of soft protons at grazing angle incidence and predict the scattered distribution. However, work has still to be done to validate and possibly improve them, being the existing experimental data not sufficient for a full comprehension of the process.

Downloaded From: https://www.spiedigitallibrary.org/conference-proceedings-of-spie on 2/28/2019
Terms of Use: https://www.spiedigitallibrary.org/terms-of-use

A setup for tests of proton reflectivity on mirror samples has been constructed at the 3 MV proton accelerator of the University of Tübingen in the past few years [7]. The current implementation allows for a sampling of the distribution of the scattered protons along the polar direction Θ, in a range of $\Phi_{scatter}$ from a few tenths of degree to a few degrees (with respect to the target surface), by means of a Si-diode movable along the axis perpendicular to the incident proton beam, as shown in Fig. 8. Some measurements have already been performed using eROSITA mirror samples as a target [7]. In the framework of the AHEAD project we are programming verification of Ir-coated targets as well. Flat samples useful for comparison of laboratory data with physical models may be prepared in house by evaporating Ir on a glass substrate, or real samples of Si-pore optics could be used. Since it is expected that protons also undergo scattering along the azimuthal direction Φ, future tests will be conducted with a modified detection system using three diodes jointly movable along the vertical axis, one in the middle to sample the on-axis polar distribution (i.e. $\Phi_{scatter}$~0) and two fixed at the sides to sample the off-axis polar distribution (e.g. at $\Phi_{scatter}$ ~1°). This should permit, in particular, a more meaningful comparison of the experimental measurements with the Remizovich's distribution [8].

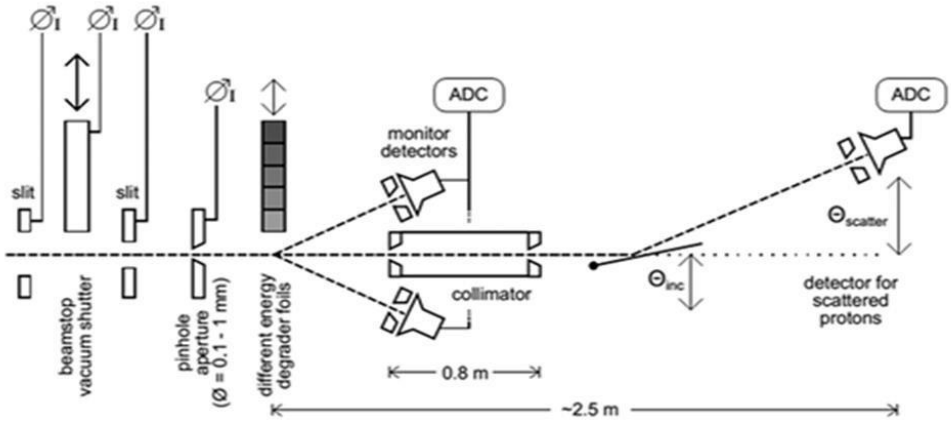

Figure 8. Schematic of the setup at the 3 MV proton accelerator of the University of Tübingen for soft proton scattering tests.

3. CONCLUSION

We presented the status of the activities at our institute with regard to the assessment of the background and optimization of the WFI camera design. Although work is still in progress, some results are already consolidated. A passivation layer deposited on the non-illuminated side of the detector is technically feasible and would effectively reduce the background level by ~30% at energies <7 keV, in the basic camera head configuration this results in a count-rate close to the requirement over the entire band. A mesh in metal, that will be used to sustain the OBF, will not have a significant impact on the continuum background, whereas a coating should be applied as a countermeasure against possible fluorescences. An internal graded shield will be used to suppress fluorescence from the Al proton shield and other sub-structures around the detector. Combining passive shielding with discarding of frames contaminated by proton trigger events, the final background level can likely be further reduced. However, we remark that in the analysis presented here we did not consider the contribution to the background that would come from environmental α-particles and electrons, as well as from substructures that will be present in the camera. We expect that these components may determine an overall increase of the background by ~20%. The possible contribution of soft protons scattered through the telescope is still an open question, however a proton diverter is foreseen, that should guarantee enough protection.

ACKNOWLEDGMENTS

This work is partially supported by the Bundesministerium für Wirtschaft und Technologie through the *Deutsches Zentrum für Luft und Raumfahrt (DLR)* under the grant number 50 QR 1401

Downloaded From: https://www.spiedigitallibrary.org/conference-proceedings-of-spie on 2/28/2019
Terms of Use: https://www.spiedigitallibrary.org/terms-of-use

REFERENCES

[1] A. Rau et al., arXiv:1308.6785,2013

[2] K. Nandra et al., arXiv:1306.2307, 2013

[3] D. Barret et al., arXiv:1307.1709 , 2013

[4] www.spenvis.oma.be

[5] M. Barbera et al., Proc. of SPIE 9601, 9601-09 (2015)

[6] Prigozhin, G. Y., Kissel, S. E., Bautz, M. W., Grant, C., LaMarr, B., Foster, R. F., and Ricker, G. R., "Characterization of the radiation damage in the Chandra x-ray CCDs" , Proc. of SPIE 4140, 123 (2000)

[7] *XMM-Newton User's Handbook*

[8] Diebold,S., Tenzer C., Perinati,E., Santangelo,A., Freyberg,M., Friedrich,P. and Jochum,J., *"Soft proton scattering measurements on x-ray mirror shells"*, Experimental. Astronomy., 39, 343-365 (2015)

[9] Remizovich,V.S., Ryazanov,M.I. and Tililin I.S., *"Energy and angular distributions of particles reflected in glancing incidence of a beam of ions on the surface of a material"*, Sov. Phys. JETP, 52, 2 (1980)

Downloaded From: https://www.spiedigitallibrary.org/conference-proceedings-of-spie on 2/28/2019
Terms of Use: https://www.spiedigitallibrary.org/terms-of-use